

The Case for Efficient and Robust RF-Based Device-Free Localization

Chenren Xu, Bernhard Firner, Yanyong Zhang, *Member, IEEE*, and
Richard E. Howard, *Senior Member, IEEE*

Abstract—Radio frequency based device-free localization has been proposed as an alternative localization technique. Unlike its active localization counterpart, it does not require subjects to wear any radio device, but tries to determine the subject's location by observing how much the subject disturbs the radio propagation patterns. This problem is very challenging due to the well known multipath effect, especially in a complex indoor environment where it is impractical to accurately model the effects of a subject on the surrounding radio links. In this article, we formulate the device-free localization problem using probabilistic classification approaches that are based on discriminant analysis. To boost the localization accuracies, we adopt methods to mitigate errors caused by the multipath effect, as well as methods to automatically recalibrate training data so that accuracy can be maintained as the environment evolves. We validate our method in a one-bedroom apartment that consists of 32 cells, using eight fixed transmitters and eight fixed receivers. When the space has a single occupant, our method can correctly estimate the occupied cell with a likelihood as high as 97.2 percent. Further, we show that we can maintain a high localization accuracy, while substantially reducing the deployment overhead, which is an important concern for device-free localization methods. To achieve this goal, we have improved our training and testing procedures to reduce the overhead, studied the radio device placement to optimize the device cost, devised algorithms to extend the lifetime of the training data, and designed a set of auxiliary sensors and incorporate them into the system to achieve automatic re-calibration.

Index Terms—Device-free localization, tracking, discriminant analysis, multipath, automatic recalibration

1 INTRODUCTION

THE past few years have witnessed a growing interest in incorporating “intelligence” in our homes and work places by using a dense array of wireless radio/sensor nodes [1]. These sensors can continuously track the locations and activities of people in indoor environments without the need for active participation of the people that are being tracked, providing a much more affordable and private solution than traditional technologies such as video camera. This trend can enable a large number of important applications, including medical care, smart energy, workflow optimization [2], and retail. For example, we can detect the onset of dementia through mobility patterns in GPS data [3] but with context sensors in the home we can detect fine-grained details about a person's welfare [4]. Human activity detection is useful to many neurological disorders, from obsessive compulsive disorder to Alzheimer's disease. The same technology can also be used to increase the comfort of healthy individuals by building “smart” homes that are aware of a person's activities. Phone calls could be muted or redirected based upon a person's current activity, energy could be conserved by heating or cooling only the

parts of a house that people are using, or the system could help parents keep track of their toddler.

All of these applications require that tracking is done automatically and unobtrusively. Radio frequency (RF) based localization techniques become increasingly popular because it offers pervasive and low cost solution, such as discussed in [5], [6], [7], [8]. These techniques usually require that users carry battery-powered wireless devices, and are thus referred to as *active* RF localization. The requirement of tagging users, however, is very inconvenient. If a system is meant to help an elderly person with memory problems then they cannot be relied upon to remember to wear a tracking device. Likewise, if a system is meant to improve the convenience of a person in their home then inconveniencing them is counter to our goal. Furthermore, wearing a tag can cause serious privacy concerns because the tag's location is always tied to the person's location.

Recognizing the mismatch between the requirements of these applications and existing solutions, we advocate using RF-based device-free localization technique is firstly proposed in [9]. In device-free localization, we capture the variation in the RF signals caused by the presence of the subject (without a radio device) and try to localize the subject based upon the observed received signal strength (RSS) variation. This does not require any action on the subject's part and does not distinguish one person from another so device-free localization is non-intrusive, convenient, and privacy preserving.

Deriving a subject's location from the RSS change caused by the subject, however, is a challenging task, mainly due to the unexpected changes in signal strength caused by the well-known “multipath” effect [10] that is caused by the

• C. Xu is with the Center for Energy-efficient Computing and Applications, School of EECS, Peking University, Beijing 100871. E-mail: chenren@pku.edu.cn.

• B. Firner, Y. Zhang, and R.E. Howard are with the Wireless Information Networks Laboratory (WINLAB), Rutgers University, North Brunswick, NJ 08902. E-mail: {bfirner, yyzhang, reh}@winlab.rutgers.edu.

Manuscript received 16 Nov. 2014; revised 14 July 2015; accepted 5 Oct. 2015. Date of publication 26 Oct. 2015; date of current version 2 Aug. 2016. For information on obtaining reprints of this article, please send e-mail to: reprints@ieee.org, and reference the Digital Object Identifier below. Digital Object Identifier no. 10.1109/TMC.2015.2493522

reflection and diffraction of RF signals from subjects and objects in the environment. Due to multipath, a subject's effect on the RSS value can seem random and unpredictable, counter to common assumptions of simple attenuation. For example, the common assumption is that the presence of a subject in a link's line of sight (LoS) leads to a reduced signal strength value, but we have observed RSS values increasing when the subject blocks the Line of Sight; the common assumption is that the impact of a subject is larger when she moves on the direct, LoS of a link compared to moving outside of the LoS, but in fact the opposite situation is also common; most radio propagation models assume that subject's impact is a smooth function of her position with respect to the link, but in fact the impact can change greatly over a small distance (e.g., a 10 dB of difference over a distance of less than 20 cm).

A few device-free localization techniques have been proposed, but they either ignored or didn't observe multipath [11], or failed to carefully consider the full range of its impacts. For example, the RSS attenuation model based radio tomography proposed in [11] tries to calculate a subject's location based upon the signal attenuation when the subject is blocking the LoS of the link. As another examples, in [12], [13], the authors assume the intersection of most affected links is the position of the subject. These schemes assume there is a direct relationship between a subject's location and the impact on radio signals, which does necessarily not hold in most indoor environments. These schemes have another potential drawback: they often require a dense deployment to generate enough radio links to cover the whole space. In [9], [14], the authors acknowledge the importance of multipath, and propose a fingerprinting-based approach in which they first collect a radio map with the subject present in a few sparse predetermined locations, and then map the test location to one of these trained locations based upon observed radio signals. While the fingerprinting approach is certainly a good fit for indoor device-free localization, the localization algorithm in [9], [14] may only fare well when the training locations are sparse and the test location closely matches one of the training locations.

In this article, we take on the challenge and aim to design a robust, accurate, and light-weight device-localization method. Considering the complexity of multipath, *we choose to adopt the fingerprinting approach, but extend it with statistical tools that fit the discrete fingerprint data so the subjects can be identified as being in random test locations not in the original training data set. The use of these fitting tools along with dense initial training data minimizes the impact of multipath.* We believe these requirements are crucial to many smart home applications such as elder care. We achieve this high performance with the following optimizations. Firstly, we formulate the localization problem into a classification problem and apply discriminant analysis based on the assumption that the covariates approximately follow a multivariate Gaussian distribution. Secondly, we have designed an extensive set of techniques that can be used to mitigate the impact of multipath, such as removing the unreliable data due to multipath in localization through our algorithm, and adopting a lower frequency. Thirdly, we have designed methods to extend the lifetime of training data over a long period to substantially reduce the training cost per

deployment and finally, we demonstrate the feasibility of reducing the number of transmitters and receivers to the minimum needed to reach a desired accuracy.

A serious challenge faced by device-free localization schemes is their seemingly high deployment overhead—it needs a relatively dense array of radio devices, as well as a large amount of manual effort (in both the training and the testing phases). Though the first factor (i.e., device cost) can be handled by carefully placing the radio devices, the second factor (i.e., manual effort) imposes much harder challenges on the system design. RF signals are sensitive to changes in the environment, and it is thus ideal to have a fresh training before each test, which, unfortunately, leads to prohibitive overhead especially considering these training sessions usually involve manual effort. In this paper, we have explored techniques that can extend the lifetime of a training session to half a year or even a year, either through correcting the training dataset by filtering out data with large variations, or through employing sensor-assisted automatic calibration. Through detailed experiments, we show that our methods can efficiently reduce the overhead, making our device-free localization efficient, robust and sustainable.

To summarize, we made the following contributions in this paper: (i) we derive a sophisticated classification model to better describe the device-free localization problem, and present different strategies (with detailed analysis) to mitigate the errors caused by the multipath (Section 2); (ii) we present the design, implementation and evaluation of our system in a one-bedroom apartment and report detailed experimental results (Section 3); (iii) we present a set of methods aiming at making our system efficient, robust and long-term sustainable with minimal human intervention, such as removing the features with corrupted data, or adding auxiliary sensors for auto-recalibration, in Section 4.

2 DEVICE-FREE LOCALIZATION THROUGH PROBABILISTIC CLASSIFICATION METHODS (PC-DfL)

Indoor radio propagation is a very complex phenomenon such that the relationship between a subject's location and her impact on the RSS of a radio link in the environment is hard to predict. Thus, statistical rather than deterministic methods are required to extract location information from the measured RF signals. In this section, we discuss in detail our proposed probabilistic classification based device-free localization method, *PC-DfL* in short.

We visualize a room as a grid of K small cells with unique addresses or ID numbers partition the deployed area into K cells. By localizing a subject, we mean to estimate accurately the ID of the cell in which the subject is located. In the training phase, we first measure the ambient RSS values for L links when the room is empty. Then a single subject appears in each cell, we take N RSS measurements from all L radio links. By subtracting the ambient RSS vector from the collected data, we have a profiling dataset \mathcal{D} . \mathcal{D} , a $K \times N \times L$ matrix, quantifies how much a single subject impacts the radio RSS values from each cell. Having this profiling dataset \mathcal{D} , *we model the subject's presence in cell i as a class S_i and thus $\mathcal{D} = \{\mathcal{D}_{S_1}, \mathcal{D}_{S_2}, \dots, \mathcal{D}_{S_K}\}$.* By the end of the training phase, we have built a K -class classifier based

on the profiling dataset \mathcal{D} . Subsequently, in the testing phase, when a subject appears in a random location, we measure the RSS values for all L links and then subtract the ambient RSS vector from this measured data, and form an RSS vector, O , which shows how much this subject impacts the radio links from this unknown cell. Based on \mathcal{D} and O , we use the classifier to classify the ID number of the unknown cell, thus localizing the subject.

2.1 Background: Discriminant Analysis Based Localization

In formulating our classification problem, we label a class i as the state with the subject in the i -th cell, and we have K classes: $\mathcal{S} = \{S_1, S_2, \dots, S_K\}$. In this problem, class S_i means the subject is located in cell i . The classifier essentially infers the current state based on the observation RSS vector O . We would like to maximize the likelihood $P(q = S_i | O, \mathcal{D})$ when cell i is occupied. In other words, when the subject is located in cell i in the testing phase, we would like to maximize the probability that the estimated cell q matches the actually occupied cell i . We apply linear discriminant analysis (LDA) [15] classifier by assuming the observed RSS vectors in each class S_i follow a multivariate Gaussian with mean μ_i and a common covariance matrix Σ , i.e., $P(O|S_i) \sim \mathcal{N}(\mu_i, \Sigma)$, as in [16]. We find

$$q = \operatorname{argmax}_i \delta_i(O),$$

where

$$\delta_i(O) = P(O|S_i).$$

We chose LDA as the supervised classification algorithm in our problem as it fits the normal distribution of the data we observed. We have compared it with different methods in our early work [17].

2.2 Mitigating Multipath Effect

The multipath effect makes indoor localization challenging and inaccurate. Therefore, we first take a closer look at indoor multipaths, and then propose two techniques that can tame the multipath effect.

While long-range radio outdoors in a complex urban environment is likely to generate many multipaths with similar powers, radio propagation behaves quite differently indoors. In an indoor environment using wavelengths of a few tens of centimeters (e.g., WiFi or cellular), there are many scatterers of similar scales (a few wavelengths in size), but there are also a few large-scale scatterers, like floors, walls, and ceilings, that produce a small number of strong reflections that can combine to create deep fades. These fades are the result of subtracting the amplitude of the radio signal, not the RSS (the log of the power), and as a result, only signals with closely matched amplitude, such as those caused by large reflection surfaces like floors, ceilings, and walls, can create a deep fade. The myriad of weaker reflections from smaller objects are far less effective at creating these deep fades [18]. The study presented in [19] looks at a distribution of reflected signals in an indoor environment, which clearly shows that only a few reflections have significant amplitude and the rest are 10 to 50 dB smaller. This causes the multipath profile indoors to be quite sparse,

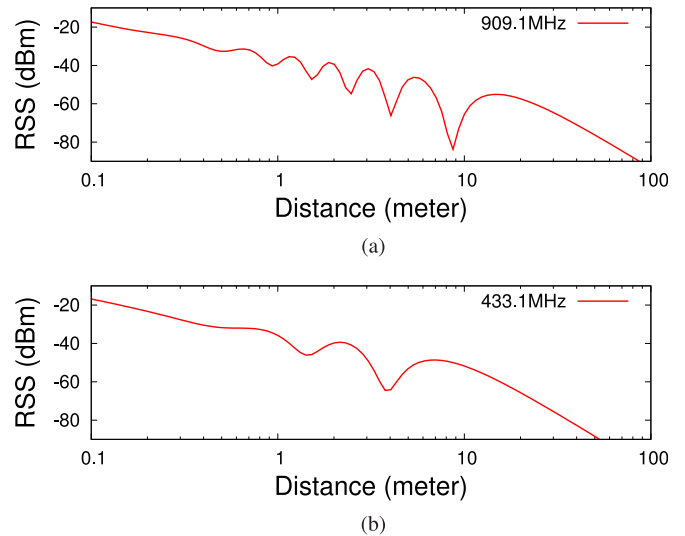


Fig. 1. The theoretical RSS values versus the distance between the transmitter and receiver. The model is evaluated at 909.1 MHz with both radios at 1.2 meters above a perfectly reflecting surface. Those “drop” are the deep fading positions. In (b), we observe fewer fades when the radio operates at 433.1 MHz.

clustered around very few paths which often correspond to large, omnipresent reflectors.

To demonstrate this effect, we plot in Fig. 1a the theoretical performance of a 909.1 MHz signal transmitted at 1mW with a single multipath (e.g., floor reflection in addition to the LoS) over an increasing distance between the transmitter and receiver, each 1.2 meters above the floor. This represents typical indoor settings such as wireless devices being placed on tables or counters. For simplicity, additional reflections from the more distant ceiling and the walls are ignored. Fig. 1a shows the resulting power calculated as the square of the sum of these two waves at each point. At nearly regular intervals, the similar amplitude and phase resulting from the two waves, LoS and the multipath, leads to a strong fade at a distance of about 13 wavelengths, a bit over 4 meters from the transmitter. Because the path lengths are only slightly different, the amplitudes are almost the same and when the phases differ by π , the difference is near zero, leading to a deep fade. Even more striking is the steepness of the drop in RSS near this fade.

We also setup a simple experiment to demonstrate both the complexity introduced by the multipath effect and the fact that a lower frequency radio help mitigate this problem. Fig. 2a shows the topology of a one-bedroom apartment in which we conduct our experiments. We have one transmitter (Tx in the picture) and one receiver (Rx in the picture), and this radio link has one Line-of-Sight (LoS) component and four Non-Line-of-Sight (NLoS) (or, multipath) components. We only show four NLoS components for simplicity; in reality there are many more present. A person walks from the marked “Start Point” to the marked “End Point”. During the movement, we record the received signal strength at the receiver (operating at 909.1 MHz), and report the differences between these values and the RSS values when the subject is absent in Fig. 2b. Fig. 2b shows that the person’s effect on the RSS value is random and unpredictable—we observe RSS decreases at different levels, and sometimes we even observe an RSS increase. Fig. 2b also shows that changes

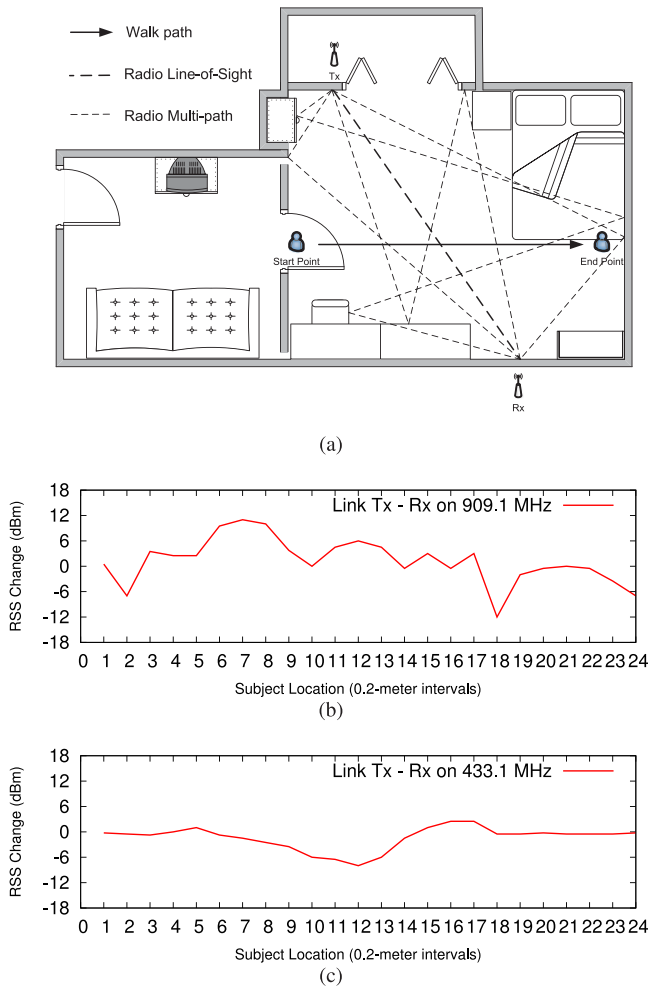


Fig. 2. (a) Shows the indoor environment in which the radio link has one LoS and four NLoS components. (b) and (c) show the fluctuation of RSS changes between Tx and Rx when the radios operate at 909.1 MHz and 433.1 MHz, respectively.

from motion relative to the LoS and NLoS components can be far larger when the subject is not on the LoS than when he is—the variation is as high as 10 db from location 17 to location 18 over a distance of less than 20 cm where the person is not crossing the LoS of the link. Finally, we note that the multipath effect is affected by many factors. Fig. 2c shows a completely different behavior when the radio frequency is set to 433.1 MHz, which has a much smoother spatial variation when people move.

Cell-based localization. Many fingerprint localization techniques are point-based ([9], [14])—fingerprints for individual points are collected in the training phase, and in the test phase the location is labeled as one of the trained point locations. This approach is very vulnerable to the aforementioned deep fades in an indoor environment. Choosing locations near fade points in the training phase can lead to large localization errors.

Instead, we propose to use a cell-based approach to reduce the risk of taking training data near fade points. We partition an indoor space into cells, and by localization we mean to identify which cell is occupied. In the training phase, we measure the RSS values when the subject is present in each of the cells; the subject makes random movements within a cell and a number of measurements are

recorded. Note that the use of cell-based fingerprinting averages over an extended region and, thus, minimizes the impact of isolated locations with deep fading. Techniques based on using only discrete points for fingerprinting, can suffer large errors from these fading points.

Radio frequency. We propose to further mitigate the impact of the multipath effect by operating radios at a lower frequency. As shown in Fig. 1b, we observe fewer and shallower fades when we operate the radio at 433.1 MHz in the theoretical curve. At lower frequencies, the wavelengths are correspondingly longer, and thus the distance between points with π phase shift is also longer. Therefore, the number of deep fades is significantly reduced over the same distance between the transmitter and receiver compared to that in the 909.1 MHz case. In the case of device-free passive localization, this intuition is captured by experimental observation in [17] as well.

3 PC-DfP DESIGN

In this section, we present in detail our system design and experimental validation effort that shows that PC-DfL can accurately localize a single subject in an indoor environment.

3.1 System Overview

Our system design of PC-DfL follows a standard layered sensing system paradigm, which is depicted in Fig. 4. It has two parts: the main part is the PC-DfL engine which streams the radio data, combines the fingerprint data, and runs the localization algorithm to determine the location, which results will be presented in the rest of this section. We will introduce the other thread, our auxiliary sensors and the associated automatic recalibration scheme with the red flow in Section 4.

3.2 Experimental Methodology

In our experiments we will show that a single subject can be successfully localized in an indoor environment using our PC-DfL method.

3.2.1 Experimental Setup

Our experimental setup consists of a host PC (Intel i7-640 LM 2.13 GHz, 3GB RAM) serving as the centralized system. In our experiments, the radio operates in the unlicensed bands at 433.1 MHz or 909.1 MHz. Radio receivers are connected to the PC through a (wireless) USB hub. We used Transmit-Only Protocol [20]—each radio transmitter broadcasts a 10-byte packet every 100 milliseconds. The receivers will forward received packets to the host PC for data collection and analysis. More detail of the system can be found in [21], [22].

The system was deployed in a one bedroom apartment with home furniture. The apartment layout is shown in Fig. 3. The apartment is below ground level with a floor area of 5×8 m and a height of 3 m. The floor is concrete, the walls are wallboard on wooden studs, and the ceiling is acoustic tile.

Radio transmitters and receivers are deployed alternatively one by one along the periphery of the wall depicted in Fig. 3. Eight transmitters and eight receivers provide

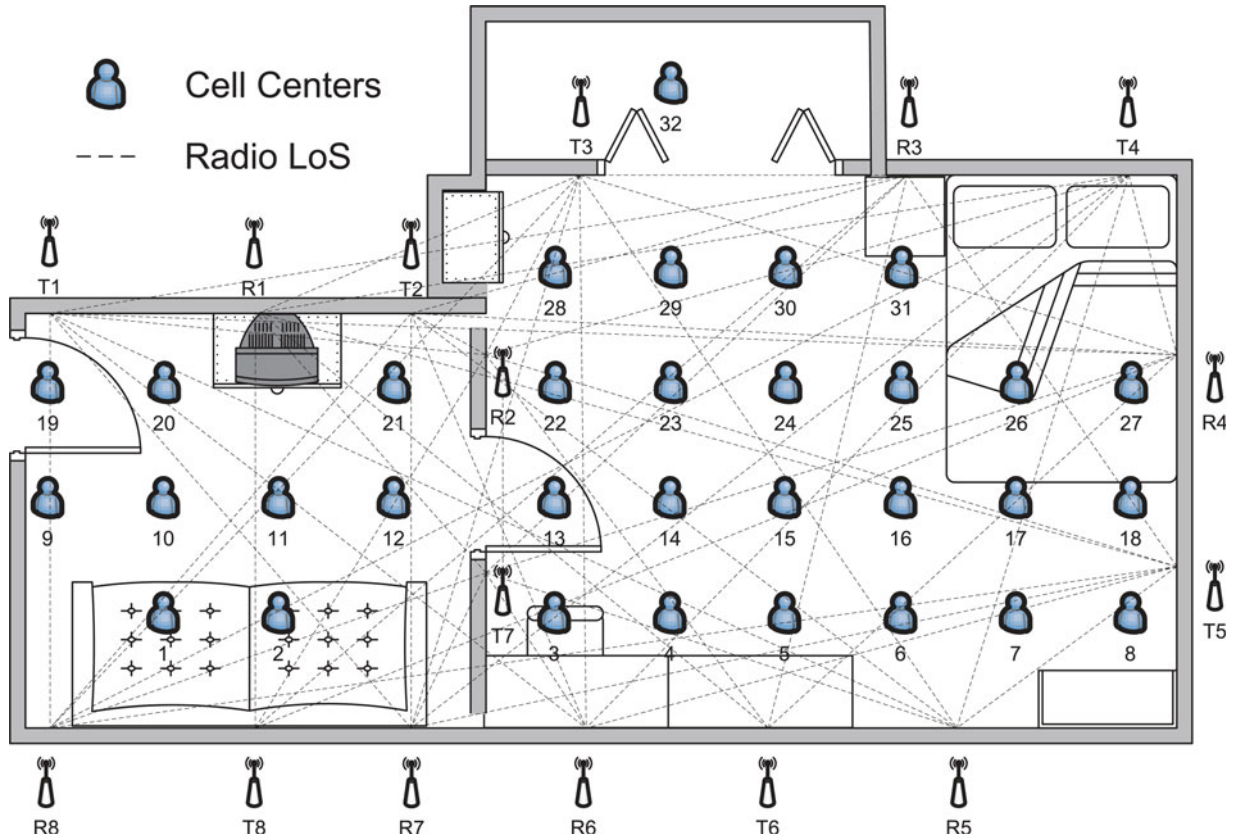


Fig. 3. We show the experimental topology. The one-bedroom deployment region is partitioned into 32 cells. The center of each cell is marked in the picture. Eight transmitters and eight receivers are deployed. We show the 64 radio Line-of-Sight links here.

64 independent radio links in total. We virtually partition the room into 32 cells, each roughly 0.75×0.75 m in size. We choose 0.75 m because it is the typical walking step size for adults. We note that a deployment of 16 nodes is relatively dense, and we will demonstrate that we only need half of them to achieve good accuracy in Section 4.

Data Collection. Our method consists of the following two phases:

- *Off-line training phase.* In the training phase, we will construct the radio map of the room by making 100 measurements in each cell (10 seconds) to determine the RSS footprint. We consider two training strategies. In the first case (*training case A*), the subject will stand at the center of each cell and spin around so that the resulting training data will focus on the cell center but involve different orientations. In the

second case (*training case B*), the subject will walk randomly within the cell. Thus, the resulting training data treat all the voxels within that specific cell uniformly and includes all possible orientations.

- *On-line testing phase.* In the testing phase, the subject (who is different from the subject in the training phase in height and weight) will appear in a random location with a random orientation. In our experiments, we have 100 test locations in each cell, resulting in a total of 3,200 test locations. Among the 100 test locations within each cell, 25 of them are the cell center, 25 of them are 0.13 m from the center, 25 of them are 0.25 m from the center, and the other 25 are 0.38 m from the center. For each test location, we take 10 RSS measurements and compute the median value for all the 64 radio links.

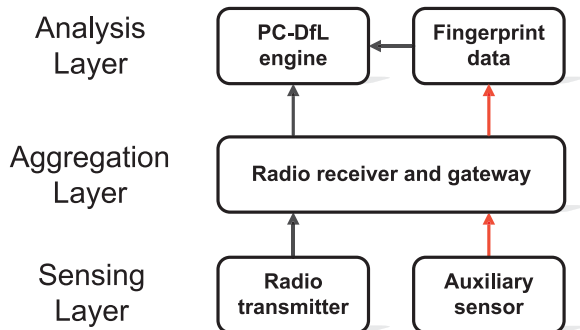


Fig. 4. System overview.

3.2.2 Deployment Cost

Unlike [11], [12], our localization algorithm does not require prior information about the locations of all the radio nodes. Transmitters and receivers can be deployed at random locations. This property ensures that PC-DfL can be applied in an environment with no changes to the existing infrastructure. In our experiments, it takes 10 seconds to collect 100 training measurements. Even considering the extra overhead of moving and turning, 30 seconds are sufficient for each cell. *Usually we spend about 15 minutes training the whole deployed region.* Given 32 cells and 100 RSS training measurements for each cell in a 64 dimensional space, it takes 44 msecs to estimate the parameters of the

TABLE 1
System Parameters

Parameter	Default value	Meaning
K	32	Number of cells
L	64	Number of radio links
N_{trn}	100	Number of training RSS vector per cell
N_{tst}	100	Number of testing RSS vector per cell

classification algorithm, and takes only 7 msec to estimate the subject location.

Overall, the runtime cost of our method is rather modest. In the latter section, we discuss ways of further reducing this cost while maintaining high localization accuracies.

3.2.3 Performance Metrics

The objective of a localization system is to maximize the likelihood of correctly estimating a subject's location and minimize the average distance between the estimated location and the actual location. For a specific test i , suppose a subject is actually located in cell y_i , and PC-DfL estimates that the occupied cell is \hat{y}_i . Further suppose we have N_{tst} tests. We thus define the following performance metrics:

- *Cell Estimation Accuracy.* Is defined as the ratio of successful cell estimations with respect to the total number of estimations, i.e., $\sum_{i=1}^{N_{tst}} I(y_i = \hat{y}_i) / N_{tst}$. In our system, we consider a test successful if the estimated cell is the same as the occupied cell. If the subject is located on the shared boundary between two adjacent cells, the test is considered successful if the estimated cell is either one of the two bordering cells.
- *Average localization error distance.* Is defined as the average distance between the actual point location of the subject and the estimated point location (i.e., the center of the estimated cell).

Table 1 summarizes the important parameters used in our experiments. To reiterate, our experiments were conducted in a one-bedroom apartment with the total area of 5×8 m, which is divided into 32 cells (size of each cell being 0.75×0.75 m). We have eight transmitters and eight receivers, resulting in 64 links in total. We note that this number can be made smaller with minimal impact on our localization results. We also note that we anticipate a reasonably large number of sensors/radio devices will be existing in a "smart" home environment. In the training phase, the experimenter stood in each of these 32 cells, and took 100 RSS measurements.

3.3 Experimental Results

We have mentioned that the multipath effect has an adverse impact on indoor localization, and in this paper, we have devised approaches to mitigate its impact for improved localization results. Specifically, due to multipath, when a subject moves around, we will observe large and abrupt RF variations, even within a cell. Therefore, accurately estimating cell ID based upon the observed RF readings becomes a daunting task. To mitigate this impact, we take the following measures to smooth out the RF variations within a cell.

TABLE 2
LDA Cell Estimation Accuracies Improve When the Radios Work on 433.1 MHz, and Adopt the Training Case B

	433.1 MHz	909.1 MHz
Training case A	90.1	82.9
Training case B	97.2	93.8

First, we operate our radios at the unlicensed frequency of 433.1 MHz instead of 909.1 MHz. Intuitively, the wavelength at 433.1 MHz (70 cm) is substantially larger than that at 909.1 MHz (33 cm), and thus the RF signal is less susceptible to multipath, fading and the presence/orientation of small objects and thus has a smoother variation when the subject is moving. We have conducted an experiment to demonstrate this idea in earlier work [17].

Second, in the training phase, instead of standing still at a specific point within a cell and using the measurement at that point to represent the entire cell (as in training case A), we make random movements within that cell, take multiple measurements, and use them collectively for classification, as in training case B in Section 3. In this way, we sample the data for all the voxels with different orientations to average out the multipath effect within each cell.

Table 2 summarizes the LDA results with and without these two optimizations. We also varied the test location in these experiments. In general, training case B gives better cell estimation accuracies than training case A. Within each training case, radio frequency of 433.1 MHz gives better results than 909.1 MHz with the node layout shown in Fig. 3. *In summary, our cell estimation accuracy is as high as 97.2 percent with the average localization error distance of 0.36 meters.* We have validated our approach in a much larger office setting of 150 m² and achieved around 1 m accuracy. More detailed could be found in our early work [17].

Finally, we want to note the reader that this fingerprinting-based approach can be easily extended with different techniques, such as demonstrated in [23], [24] and to address the problem of localizing multiple people.

4 EFFICIENT AND ROBUST PC-DfL

Though we have shown that PC-DfL can accurately localize subjects, it suffers from high deployment overhead, in both manual effort in calibration and testing as well as device cost. In this section, we thus devise schemes to tackle this challenge and show that we can retain localization accuracies while significantly reducing the overhead. As a result, our PC-DfL scheme will be efficient, robust and sustainable.

Specifically, we would like to answer the following important questions: (1) Given a desirable training dataset size, can we reduce the overhead in both training and testing when performing PC-DfL? (2) Can we reduce the number of radio nodes needed to deliver a reasonable localization accuracy? (3) Can we use the same training data over a long testing period with through lightweight re-calibration?

4.1 Reducing Training/Testing Overhead

Here we investigate methods for reducing the computing overhead for our algorithm. In this study, we formulate the localization problem as a classification problem that

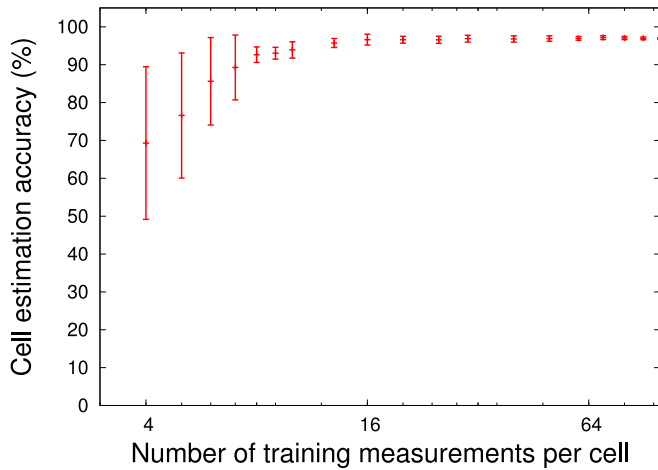


Fig. 5. The 95 percent confidence interval error bar shows that we can achieve 90 percent cell estimation accuracy only using 16 training measurements.

involves a training phase and a testing phase. Suppose we have N training data of L dimensions and K classes, where N is the number of measurements taken in each cell in the training phase, L is the number of radio links in the environment, and K is the number of the cells in the environment. In our default setting, we have $N = 100$, $L = 64$, and $K = 32$.

For LDA, the algorithmic complexity is $O(KNL + K^3)$ in the training phase and $O(KL^2)$ in the testing phase. As K is fixed in our algorithm, we can try to use a smaller N and/or L to reduce the overhead.

First, we look at the possibility of having a smaller N , i.e., fewer training samples. Fig. 5 shows the localization results with different training data sizes. We observe that we achieve a cell estimation accuracy of at 90 percent by using 16 training measurements in each cell, and achieve a cell estimation accuracy as high as 90 percent by only using eight training measurements in each cell. This will lead to a significant reduction of the training overhead.

Next, we look at the possibility of having a smaller L , i.e., smaller data dimensions. To do so, we adopt Fisher-LDA [15] to select the principal discriminant components for classification purpose and, thereby, remove some of the redundancies in the feature space. Fig. 6 shows that we can

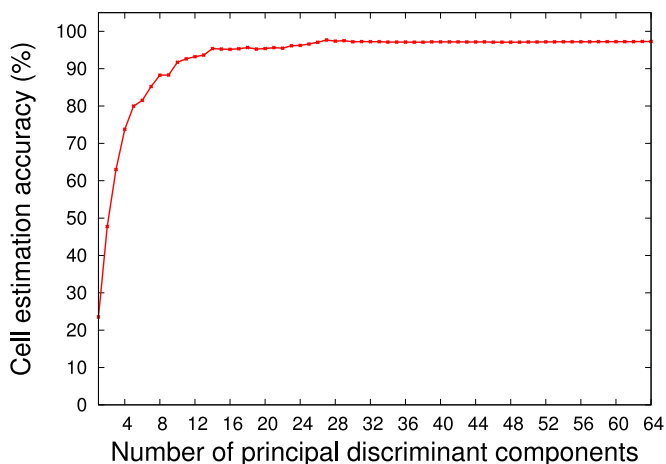


Fig. 6. Cell estimation accuracy as a function of the number of most important principal discriminant components.

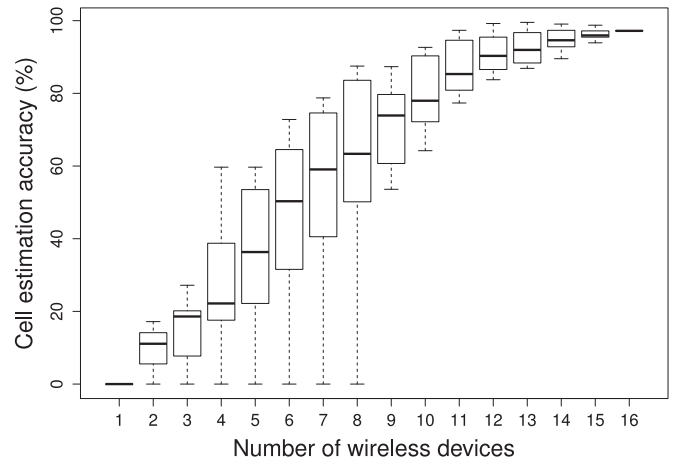


Fig. 7. Boxplot shows we can use only eight transmitters and receivers to achieve as high as 90 percent cell estimation accuracy.

achieve the same level of cell estimation accuracy when using only the first 28 principal discriminant components. Such a reduction of data dimension can lead to significant improvement on computation efficiency. If we are willing to relax the requirements for the cell estimation accuracy from 97 percent down to 90 percent, then choosing the 10 most principal discriminant components will be sufficient. These cases are implying some redundancies in the feature space, which leads to the topic of optimizing the sensor deployment.

4.2 Optimizing Radio Node Deployment

In the previous experiments, we have had a uniform node deployment: we attach the radio transmitters and receivers alternatively one by one with approximately the same distance between them. This deployment guarantees all the cells are “evenly” covered by the same number of radio LoS links. In other words, when an arbitrary cell is occupied, there are always a few radio links that are affected. In this section, we would like to investigate whether we can improve the deployment efficiencies. Specifically, we would like to find out whether we can use fewer nodes, whether the number of links affects localization accuracies, and whether the length of a link affects our accuracies.

4.2.1 Minimizing Number of Radio Nodes

A typical localization algorithm needs to trade off between tracking accuracy and deployment cost. Given a desired accuracy level, we would like to find out the lowest number of nodes we need. For this purpose, we use a subset of the radio nodes in our experiments and derive the corresponding localization results, and observe at what point the cell estimation accuracy will drop below a tolerable level. For example, if we would like to find out the results using eight radio devices out of the default 16 (eight transmitters and eight receivers), we would systematically remove all subsets of eight devices, and plot the localization results for all the possible combinations of eight transmitters and receivers.

These results are shown in Fig. 7. We find that our algorithm can deliver a cell estimation accuracy as high as 90 percent when we happen to remove the “worst” three transmitters and five receivers. In addition, we note that our system can achieve an even better accuracy (than having all 16

nodes), 99.4 percent, when three particular devices (i.e., T7, R4 and R6) are removed. Note that we do not reposition the remaining nodes to optimize the results, so this is an overestimate of the number of nodes needed for a given accuracy. Finally, we notice that we can have as high as 97 percent cell estimation accuracy with use 11 nodes (in a case we remove three receivers and two transmitters), which suggests that we can save more receivers than transmitters, the most cost-efficient choice for removing redundancies.

4.2.2 Ranking Features

Feature formulation is critical in a classification problem. In PC-DfL, features are radio links, which are directly determined by the placement of radio nodes. Intuitively, each radio link contributes differently to estimating an occupied cell depending upon the distance from that cell to the link as well as the link's LoS length. Next, we will take a closer look at these two properties and understand their bearings on localization accuracies.

The first step is to choose a proper parameter to measure how far away a cell is from a radio link. We adopt the parameter model proposed in [25]. For an arbitrary link i between transmitter T and receiver R , consider an ellipse with foci at T and R when the subject is at cell k . We define

$$\lambda_i^k = d(T, k) + d(R, k) - d(T, R),$$

where d measures the physical distance between T and R . In other words, the parameter λ is equal to the major diameter of an ellipse passing through cell k with foci at the two nodes of link i , minus the LoS length of link i . An alternative parameter could be λ' , the perpendicular distance from the cell center to the line between T and R , or λ'' , the distance from the cell center to the midpoint of the line segment between T and R . Among these three parameter models, λ is the most robust against errors. For instance, if a subject is located at the extended line of a line segment, we have $\lambda' = 0$, but in this case, the subject is actually away from that link. Another example will be when a subject is close to either the transmitter or the receiver, we have $\lambda'' = \frac{1}{2}d(T, R)$, while the subject is close to the link enough to block its LoS.

To better understand how λ is related to the cell estimation accuracy, we consider all the cells and report the result in an average manner. In other words, for each cell k , we calculate λ_i^k for all the radio links, and group them into different bin intervals. For any bin b , we denote λ_b as all the λ_i^k inside bin b . For each cell k , we remove all the links with λ_i^k in a specific bin, and compute the cell estimation accuracy for cell k , denoted as CEA_k . We compute

$$CEA_{\lambda_b} = \sum_{k=1}^K CEA_k / K.$$

Let CEA_0 be the cell estimation accuracy with the complete set of radio links, the importance of λ_b can be measured by F-score:

$$F_b = \frac{CEA_0 - CEA_{\lambda_b}}{CEA_0}.$$

A positive F-score suggests that the chosen features contribute to the localization accuracy. In our deployment, the value of λ ranges $[0, 8)$. We plot our F-score results based on different bin size 2 and 4. Fig. 8a shows that when the bin size is chosen as 2, the F-score for each bin is positive, even for those λ values between 6 and 8, which further confirms the complexities of the multi-path effect. In addition, compared with other bins, if we remove the links with λ between 2 and 4, the localization accuracy will significantly reduce. If we have an even split, Fig. 8b shows that we will lose nearly 40 percent of the localization accuracy when the links with λ less than 4 are removed, while the effect of removing the links with λ greater than 4 is negligible. These results show that the most relevant links to a cell are neither too near to nor too far away from the cell—if the link is too close, its RSS is overly sensitive to the subject's movement; when a link is too far away, the subject's impact on its RSS is negligible.

A link's LoS length (the physical distance between transmitter and receiver) is another important parameter to study. Fig. 8b suggests that for each cell, links with $\lambda < 4$ are much more important than the rest. Therefore, we conduct a feature ranking study based upon this parameter among those links with $\lambda < 4$. We group these links into bin intervals of size 2, perform the same procedure as above, and plot the results in Fig. 8c. We find that links whose LoS length is between 2 and 6 are much more important than the others. This result is also rather intuitive: short links are not often cut through by the subject's movement, thus do not contribute to localizing the subject, while long links have less RSS variation.

4.3 Using the Same Training Set Over a Long Testing Period

All the results shown above have the testing phase done within three days after training the system. In reality, we are also interested in knowing how well our system will perform if the testing occurs at a much later time, which could lead to performance degradation because of changes in the environment or drift in the radio. Different subjects or changes in the same subject could also affect the results.

All the above factors can change the relevance of the original RSS calibration and training. Thus, we need to find an effective correction technique to extend the accuracy of an original calibration over weeks or months. The basic idea is that before each experiment, be it training or testing, we always collect the environmental RSS vector RSS_E when the room is unoccupied. We refer to this vector as RSS_E^{trn} and RSS_E^{stst} for the training and testing phase respectively. This information provides the correction basis for the test data. We can determine when to collect RSS_E^{stst} based upon the subject's life style. For example, it can be collected at noon if he/she works regularly, or at midnight if he/she stays home most of the time.

Using the environmental RSS vector, we propose the following two correction approaches:

- Naive correction: For a simple correction accounting for change over time, we first compute the pairwise difference between the RSS_E^{trn} and RSS_E^{stst} , and record the vector as RSS_E^{bias} . Then we add this bias

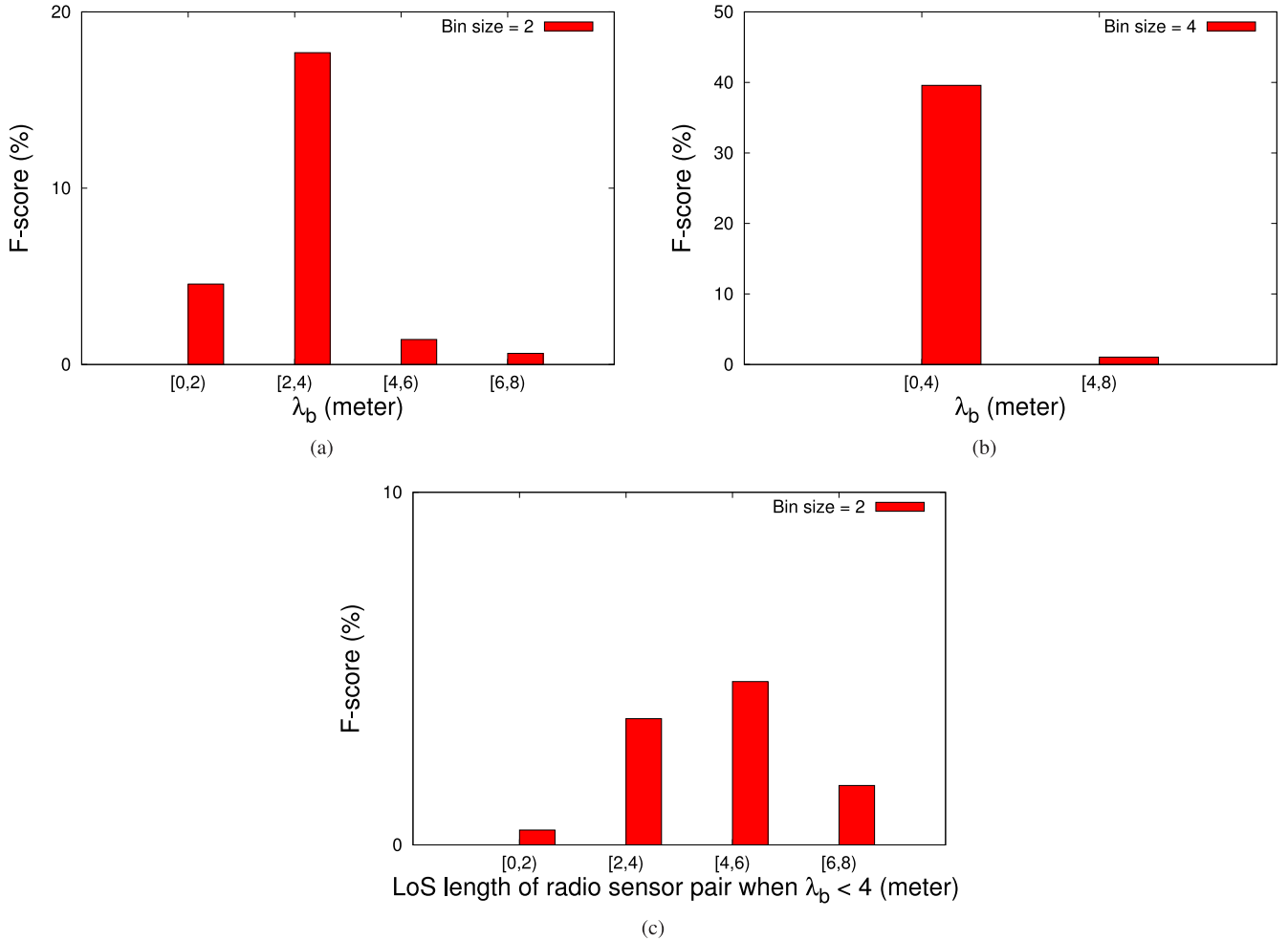


Fig. 8. The F-scores when different feature sets are removed in the original problem. (a) and (b) demonstrates that the features closer to localized subject contribute more to the localization accuracy. (c) shows that among the features with $\lambda_b < 4$ meter, the radio links with length between 2 and 4 meter contribute more than the rest.

vector to each RSS vector as the compensation and construct the new test data.

- Truncated correction: We compute RSS_E^{bias} as with naive correction and set an empirical threshold τ . Then we compare the i th entry $RSS_E^{bias_i}$ with τ for $i \in 1, \dots, L$. If $|RSS_E^{bias_i}| \geq \tau$, then we eliminate that feature (link) from both training data and test data. Otherwise, we compensate the test data for that feature as in naive correction. The rationale behind this approach is that we want to eliminate those links that have experienced a large variation due to environmental instabilities. Since our earlier results (Fig. 7) show that our system is robust against missing a few links, we believe removing these links with large fluctuation will not significantly degrade the performance.

We summarize the results in Fig. 9. In the case without correction, we do not subtract the environmental RSS from the training/test data. The results show that cell estimation accuracies drop significantly one week after training the system without any correction. With naive correction, we can achieve a cell estimation accuracy of 80 percent after one month, and truncated correction provides 90 percent cell estimation accuracy after one month, which is the best among all three.

4.4 Automatic Re-Calibration Through Auxiliary Sensors

According to our earlier discussion, in order to compensate for the errors introduced by environmental changes, we need to take away those radio links whose RSS values are no longer invalid due to the changes. In this fashion, we

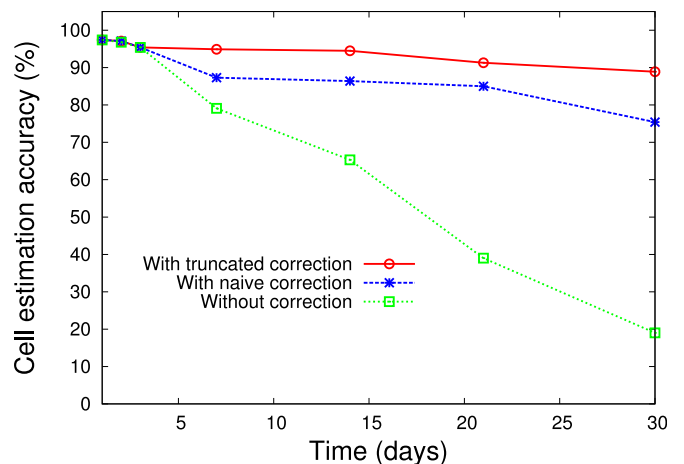


Fig. 9. With truncated correction, cell estimation accuracy remain as high as 90 percent in the test conducted one month later.

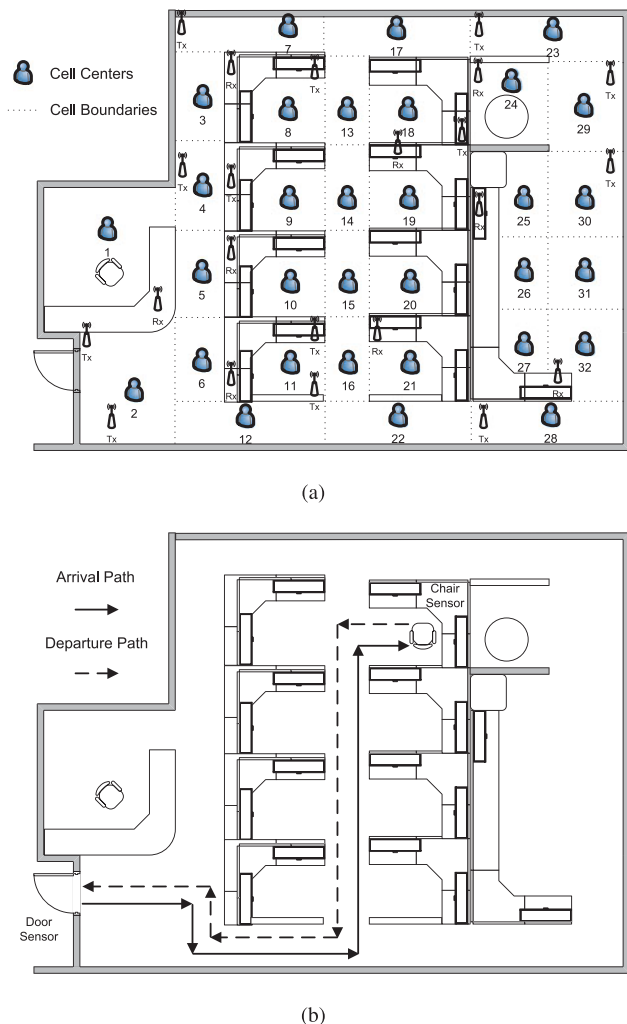


Fig. 10. In (a), we show the experimental topology. The office deployment region is partitioned into 32 cubicle-sized cells. Thirteen transmitters and nine receivers are deployed. We show the cell boundaries in this plot. In (b), auxiliary sensors are deployed on the door and chair to achieve long-term automatic recalibration.

may lose too many the radio links as we proceed, leading to a time limit on the utility of a specific calibration data set. To extend the useful lifetime of a calibration data set, we need to design a method that can automatically recalibrate the training data as the environment evolves.

In this section, we use our deployment in the university office/laboratory to demonstrate the automatic recalibration method. We deploy 13 transmitters and nine receivers in this office of 10×15 m in size. In such an environment, localizing subjects at a 0.75×0.75 m cell granularity is not needed; instead, a cubicle-size cell should be sufficient. Thus, we can still partition the deployed area into 32 cells. This deployment has two main differences compared to our original deployment: heterogeneous cell sizes and random radio positions (i.e., not always on the walls), as shown in Fig. 10a. We believe these differences make this setting more generic and challenging, and therefore we used this deployment for our experiments in this section. Using the same method described in Section 2, our cell estimation accuracy is 93.8 percent and the average localization error distance is 1.3 m. This degradation compared to the performance in the one-bedroom apartment can be explained as

follows. Intuitively, a larger cell involves more voxels, which result in a large variance for each class. Therefore, for all the classes, there is a higher probability that each pairwise class will have a larger intersection area, which leads to more classification error.

We notice that in this deployment, people spend most of their time sitting on the chairs. When moving, they usually follow a fixed path between the door and the chair and do not walk through walls, as illustrated in Fig. 10b. In the vision of “Internet-of-Things”, each object will have a sensor attached which not only but also make this information available to the Internet applications. Assuming each door and chair has a sensor, and based on the sensory data, we can obtain the times at which they open the door or they occupy the chair. Consequently, we can measure the RSS values at these times, as well as the RSS values between these events, estimate the subject’s location (based upon the fixed path and the assumption of a fixed walking pace) accordingly, and update the training data. We refer to this process as *automatic recalibration*.

To implement automatic recalibration, we made chair sensors and door sensors (shown in Figs. 12a and 12b respectively) to record the time window during which the chair is occupied and the time when the door is opened. Both of these sensors operate in a similar manner. The sensor sends power from a output pin on the microcontroller and into a wire that connects to an input pin on the microcontroller. The wire is interrupted by a switch – if the switch is closed then the input pin has logical “one” signal, but if the switch is open, the input has a logical “zero”. For chair sensors we used physical switches attached to the bottom of chairs that are switched on or off by the weight of a person sitting on the chair. For door sensors we used a magnetic switch that is closed when a magnet attached to the door is close to the switch. This is the same type of switch commonly used in home security systems. Both chair sensors and door sensors send beacons indicating their status to the system once every second. Once the status changes (e.g., the door is opened, or the chair is occupied/emptied), the system will be notified with a maximum latency of 1 second.

A typical path between the door and the chair is shown in Fig. 10b. In our test, we use the training data collected six months ago, and we try to show that these auxiliary sensors can achieve desirable localization accuracies using the same training data. For this purpose, we conduct the following four tests:

- *Test 1.* The subject follows the *arrival path* (the path between the door and the chair) and the system will track that subject based on the training data collected six months ago. Meanwhile, the system will collect more data (10 samples per cell for those cells on the subject’s arrival path), and replace part of the training data (original training data contains 100 samples per cell) with the “fresh” data.
- *Test 2.* The subject follows the *departure path* (the path between the chair and the door). The system tracks the subject using the training data after *Test 1*, and at the same time collect more RSS samples. As a result, at the end of this test, each cell on the path (we assume the departure path and arrival path consist

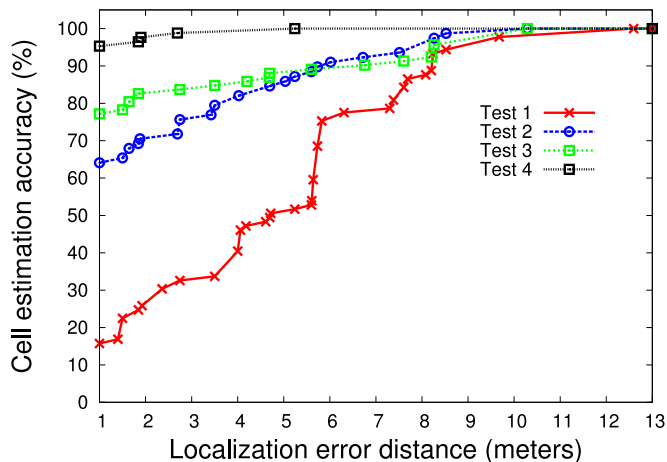


Fig. 11. Localization accuracy is significantly improved through automatic recalibration with auxiliary sensors.

of the same set of cells, but in opposite orders) now contains 80 samples collected six months ago, and 20 fresh samples.

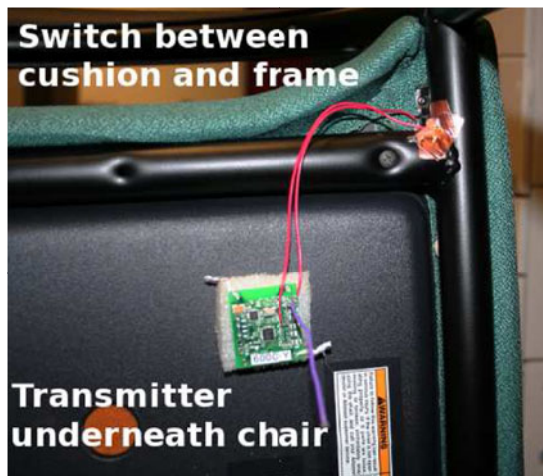
- *Test 3.* The subject follows the *arrival path*. The system tracks the subject using the training data after the first two tests, and at the same time collect more RSS samples. At the end of this test, each cell on the path contains 70 samples collected six months ago, and 30 fresh samples.
- *Test 4.* The subject follows the *departure path*. The system tracks the subject using the training data after the first three tests, and at the same time collect more RSS samples. At the end of this test, each cell on the path contains 60 samples collected six months ago and 40 fresh samples.

We plot our results in Fig. 11. We observe that after 6 months, the environmental change has led to poor localization accuracies if we use the same training data. *Test 1* yields a cell estimation accuracy of 15.5 percent. However, benefiting from the automatic recalibration from *test 1*, we achieve a much better accuracy in *test 2*. We achieve 65 percent of cell estimation accuracy when we only update 10 percent of the training data after 6 months. In *test 3* and *test 4*, we see that our localization accuracies keep improving with more updates. *Test 4* can achieve a cell estimation accuracy of 95 percent with 30 percent of updated training data.

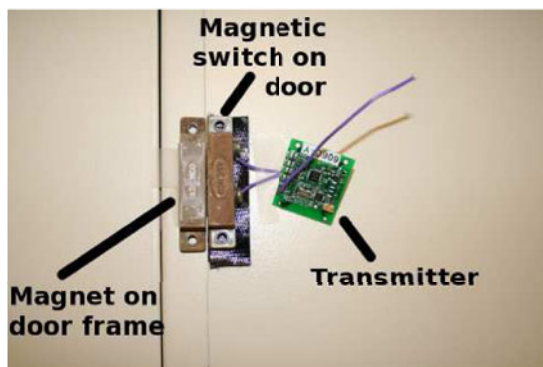
One interesting observation is that, the performance of *test 3* is slightly worse than that of *test 2* in the localization error distance between 6 and 9 m. This is because this test is conducted based on the training data updated from *test 1* and *test 2*, with reverse trajectories and subject orientation. When human subjects change their orientation in a cell, the RSS will change correspondingly because they change the parameters in diffraction and shadowing models.

We show the cell estimation accuracy and average localization error distance in Table 3. Overall, when we use partially updated training data with the same path up to three times, we can successfully track a subject moving trajectory with almost 95 percent cell estimation accuracy and 1 m error distance.

We would like to point out that, it is also possible to facilitate this automatic recalibration procedure, such as discussed in [26]. However, we note that not all the office/home



(a)



(b)

Fig. 12. These modified pipsqueak tags act as sensors. Figure (a) shows switch sensors used in chairs, and Figure (b) shows them attached to doors.

residents will be comfortable with having a camera installed due to privacy concern by nature.

5 RELATED WORK

In this section, we discuss the related work of device-free tracking techniques, which can be categorized into two main streams:

Device-free location determination. In this category, the goal is to find human subjects' location. In [9], [14], [27], [28], Device-free localization is done through fingerprint matching methods. A passive radio map is constructed during the training phase by recording RSS measurements with a subject standing at pre-determined locations. During the testing phase, the subject appears in random locations, and the system can match the observed RSS readings to the RSS readings from one of the trained locations based upon

TABLE 3
Localization Results with Automatic Recalibration over Time

Different Test Path	Cell Estimation Accuracy (%)	Average Localization Error Distance (m)
Test 1	15.5	4.7
Test 2	64.3	2.3
Test 3	77.8	2.1
Test 4	94.8	1.1

probabilistic matching algorithms. Our method shares the same philosophy with [9], [27] in that multipath is so complex that we cannot understand the direct relationship between a subject's location and the radio signal changes from one channel. Instead, we have to train the system first. We have taken special care by using stochastic fingerprinting and lower radio frequency in the training phase to minimize the RF signal variation within short distances to mitigate the multipath effect. These measures are based upon our in-depth understanding of the radio propagation properties and can lead to much improved localization results. This probabilistic approach has also been demonstrated with better results in a much larger setting with WiFi infrastructure [14] as well because more samples will better characterize the radio environment.

Radio tomography imaging (RTI) [11] is a technique to estimate the changes in the RF propagation field of the monitored area, assume the pixels with changing values are subjects' location, and then forms an image of the changed field. Here, the authors assume that the relationship between a subject' location and the radio signal variation can be mathematically modeled. In [11], [25], based upon the shadowing effect (RSS is attenuated when the LoS is blocked) caused by the subject, a linear attenuation model and a Sequential Monte Carlo model are proposed respectively. This technique is unlikely to fare well in a cluttered indoor environment because we observed that a person blocking the LoS can only attenuate the RSS with a 50 percent probability as observed in [17]. Other recent work based this framework have been proposed to use kernel distance between between a short-term histogram and a long-term histogram [29], quantify the radio links characteristics based on different fade levels [30], multiple channels [31] to average and compensate the large variation of relating the changes in the RSS to the pixel in their model. However, as an intrinsic property, radio tomographic imaging techniques require a relatively dense deployment—one node every 2 or 3 m², while our approach only require one node every 5 m² to achieve similar accuracy.

Device-free motion tracking. Another branch of approaches have been proposed to track human subjects' motion based on the RF based measurements in a passive fashion. In [12], [32], a grid sensor array is deployed on the ceiling for the tracking purpose. An "influential" link is one whose RSS change exceeds a empirical threshold. The authors calculate a subject's location based upon the observation that these influential links tend to cluster around the subject. This work is extended in [33] with triangle sensor array deployment and training information. VRTI [13], leverage the RSS dynamics caused by the moving subject under the RTI framework to generate a radio tomographic motion imaging for tracking mobile subjects' location. In [34], [35], the authors used the RSS variance and adopt a online recalibration method to maintain high accuracy of motion detection in a long run. Their focus are different from ours in that we aim to localize a person no matter (s)he is in motion or not. Adib et al. designed and implemented a USRP based software-defined radio approach by introducing a FMCW radar to track body motion via radio reflections [36]. Their approach can achieve centimeter accuracy by at the cost of relatively expensive hardware. We want to point out again

that although these approaches achieved good accuracies, they require a dense deployment, either from ceilings or stands, which are not always feasible in many monitored areas. Besides these techniques on location tracking, there are recent interests in tracking applications in a device-free fashion. For example, recently work [37] have shown that it is possible to use one or multiple links to locate and monitor human breathing using RTI. E-eyes [38] use CSI measurements to achieve a finer-grained motion detection and further profile different home activity based on the trajectory of the location.

Finally, we would like to point out that not only fingerprint-based schemes (including ours) need a training phase, but other techniques such as radio tomography and grid sensor array also need a training phase to determine a number of calibration parameters due to the very different nature of radio propagation in different environments, to detect if a subject is on the radio LoS. In addition, some recent work [39] has demonstrated that it is possible to use 3D ray-tracing techniques enhanced by the uniform theory of diffraction to model the electric field behavior and the human shadowing effect, thus to generate the passive radio map without manual calibration effort.

6 CONCLUSION

In this article, we present the design, implementation, and evaluation of PC-DfL, a device-free passive localization method based on probabilistic classification. Through extensive experiments, we validate that linear discriminant analysis is a satisfactory algorithm to solve this problem. We also propose ways of mitigating the error caused by multipath effect for better localization results, and demonstrate approaches for automatic recalibrating training data to improve the accuracy of tests made much later than the original training without manual calibration manually. We evaluate our method in a real home environment, rich in multipath. We show that our system can successfully localize a subject with 97 percent cell estimation accuracy within 0.36 m error distance. Through detailed experiments, we demonstrate that our method can achieve a basic accuracy of over 97 percent. More importantly, it can maintain an accuracy of over 90 percent with a substantial reduction in number of radio devices (from 16 down to 8), with far fewer training samples (from 100 to only 16 per cell). We can further extend the lifetime of the training data to the duration of a month while keeping the cell estimation accuracy above 90 percent. Finally, we design a set of auxiliary sensors and incorporate them into the system to achieve automatic re-calibration over a long-term period and significantly improve the localization accuracy without manual re-calibration effort.

ACKNOWLEDGMENTS

Chenren Xu is the corresponding author.

REFERENCES

- [1] (2009). Sensors help keep the elderly safe, and at home [Online]. Available: <http://www.nytimes.com/2009/02/13/us/13senior.html>
- [2] H. M. Khoury and V. R. Kamat, "Evaluation of position tracking technologies for user localization in indoor construction environments," *Autom. Construction*, vol. 18, no. 4, pp. 444–457, 2009.

- [3] N. Shoval, G. K. Auslander, T. Freytag, R. Landau, F. Oswald, U. Seidl, H.-W. Wahl, S. Werner, and J. Heinek, "The use of advanced tracking technologies for the analysis of mobility in alzheimer's disease and related cognitive diseases," *BMC Geriatrics*, vol. 8, no. 7, 2008, pp. 7–18.
- [4] J. Biswas, K. Sim, W. Huang, A. Tolstikov, A. Aung, M. Jayachandran, V. Foo, and P. Yap, "Sensor based micro context for mild dementia assistance," in *Proc. 3rd Int. Conf. Pervasive Technol. Related Assistive Environ.*, 2010, p. 20.
- [5] P. Bahl and V. Padmanabhan, "Radar: An in-building Rf-based user location and tracking system," in *Proc. 19th Annu. Joint Conf. IEEE Comput. Commun. Soc.*, 2000, pp. 775–784.
- [6] N. B. Priyantha, A. Chakraborty, and H. Balakrishnan, "The cricket location-support system," in *Proc. 6th Annu. Int. Conf. Mobile Comput. Netw.*, 2000, pp. 32–43.
- [7] D. Madigan, E. Einahrawy, R. Martin, W.-H. Ju, P. Krishnan, and A. S. Krishnakumar, "Bayesian indoor positioning systems," in *Proc. 24th Annu. Joint Conf. IEEE Comput. Commun. Soc.*, 2005, pp. 1217–1227.
- [8] K. Chintalapudi, A. Padmanabha Iyer, and V. N. Padmanabhan, "Indoor localization without the pain," in *Proc. 16th Annu. Int. Conf. Mobile Comput. Netw.*, 2010, pp. 173–184.
- [9] M. Youssef, M. Mah, and A. Agrawala, "Challenges: Device-free passive localization for wireless environments," in *Proc. 13th Annu. Int. Conf. Mobile Comput. Netw.*, 2007, pp. 222–229.
- [10] T. Rappaport, *Wireless Communications: Principles and Practice*, 2nd ed. Englewood Cliffs, NJ, USA: Prentice-Hall, 2001.
- [11] J. Wilson and N. Patwari, "Radio tomographic imaging with wireless networks," *IEEE Trans. Mobile Comput.*, vol. 9, no. 5, pp. 621–632, May 2010.
- [12] D. Zhang, J. Ma, Q. Chen, and L. M. Ni, "An RF-based system for tracking transceiver-free objects," in *Proc. 5th Annu. IEEE Int. Conf. Pervasive Comput. Commun.*, 2007, pp. 135–144.
- [13] J. Wilson and N. Patwari, "See-through walls: Motion tracking using variance-based radio tomography networks," *IEEE Trans. Mobile Comput.*, vol. 10, no. 5, pp. 612–621, May 2011.
- [14] M. Seifeldin, A. Saeed, A. E. Kosba, A. El-Keyi, and M. Youssef, "Nuzzer: A large-scale device-free passive localization system for wireless environments," *IEEE Trans. Mobile Comput.*, vol. 12, no. 7, pp. 1321–1334, Jul. 2013.
- [15] T. Hastie, R. Tibshirani, and J. H. Friedman, *The Elements of Statistical Learning*, 2nd ed. New York, NY, USA: Springer, 2003.
- [16] C. Xu, B. Firner, Y. Zhang, R. Howard, and J. Li, "Statistical learning strategies for RF-based indoor device-free passive localization," in *Proc. 9th ACM Conf. Embedded Netw. Sens. Syst.*, 2011, pp. 365–366.
- [17] C. Xu, B. Firner, Y. Zhang, R. Howard, J. Li, and X. Lin, "Improving RF-based device-free passive localization in cluttered indoor environments through probabilistic classification methods," in *Proc. 11th Int. Conf. Inf. Process. Sens. Netw.*, 2012, pp. 209–220.
- [18] W. U. Z. Bajwa, "New information processing theory and methods for exploiting sparsity in wireless systems," Ph.D. dissertation, Univ. Wisconsin-Madison, Madison, WI, USA, 2009.
- [19] D. Cassioli, M. Win, and A. Molisch, "A statistical model for the UWB indoor channel," in *Proc. IEEE Veh. Technol. Conf.*, 2001, pp. 1159–1163.
- [20] B. Firner, C. Xu, R. Howard, and Y. Zhang, "Multiple receiver strategies for minimizing packet loss in dense sensor networks," in *Proc. 11th ACM Int. Symp. Mobile Ad Hoc Netw. Comput.*, 2010, pp. 211–220.
- [21] R. S. Moore, B. Firner, C. Xu, R. Howard, Y. Zhang, and R. Martin, "Building a practical sensing system," in *Proc. IEEE Int. Conf. IEEE Cyber, Physical Social Comput. Green Comput. Commun., Internet Things*, 2013, pp. 693–698.
- [22] R. S. Moore, B. Firner, C. Xu, R. Howard, R. Martin, and Y. Zhang, "It's tea time: Do you know where your mug is?" in *Proc. 5th ACM Workshop HotPlanet*, 2013, pp. 63–68.
- [23] C. Xu, B. Firner, R. S. Moore, Y. Zhang, W. Trappe, R. Howard, F. Zhang, and N. An, "SCPL: Indoor device-free multi-subject counting and localization using radio signal strength," in *Proc. 12th Int. Conf. Inf. Process. Sens. Netw.*, 2013, pp. 79–90.
- [24] I. Sabek, M. Youssef, and A. V. Vasilakos, "Ace: An accurate and efficient multi-entity device-free WLAN localization system," *IEEE Trans. Mobile Comput.*, vol. 14, no. 2, pp. 261–273, Feb. 2015.
- [25] X. Chen, A. Edelstein, Y. Li, M. Coates, M. Rabbat, and A. Men, "Sequential Monte Carlo for simultaneous passive device-free tracking and sensor localization using received signal strength measurements," in *Proc. 10th Int. Conf. Inf. Process. Sens. Netw.*, 2011, pp. 342–353.
- [26] C. Xu, M. Gao, B. Firner, Y. Zhang, R. Howard, and J. Li, "Towards robust device-free passive localization through automatic Camera-assisted recalibration," in *Proc. 10th ACM Conf. Embedded Netw. Sens. Syst.*, 2012, pp. 339–340.
- [27] M. Seifeldin and M. Youssef, "A deterministic large-scale device-free passive localization system for wireless environments," in *Proc. 3rd Int. Conf. Pervasive Technol. Related Assistive Environ.*, 2010, p. 51.
- [28] H. Aly and M. Youssef, "An analysis of device-free and device-based WiFi-localization systems," *Int. J. Ambient Comput. Intell.*, vol. 6, no. 1, pp. 1–19, Jan. 2014.
- [29] Y. Zhao, N. Patwari, J. M. Phillips, and S. Venkatasubramanian, "Radio tomographic imaging and tracking of stationary and moving people via kernel distance," in *Proc. 12th Int. Conf. Inf. Process. Sens. Netw.*, 2013, pp. 229–240.
- [30] O. Kaltiokallio, M. Bocca, and N. Patwari, "A fade level-based spatial model for radio tomographic imaging," *IEEE Trans. Mobile Comput.*, vol. 13, no. 6, pp. 1159–1172, Jun. 2014.
- [31] M. Bocca, O. Kaltiokallio, N. Patwari, and S. Venkatasubramanian, "Multiple target tracking with RF sensor networks," *IEEE Trans. Mobile Comput.*, vol. 13, no. 8, pp. 1787–1800, Aug. 2014.
- [32] D. Zhang and L. M. Ni, "Dynamic clustering for tracking multiple transceiver-free objects," in *Proc. IEEE Int. Conf. Pervasive Comput. Commun.*, 2009, pp. 1–8.
- [33] D. Zhang, Y. Liu, and L. Ni, "RASS: A real-time, accurate and scalable system for tracking transceiver-free objects," in *Proc. IEEE Int. Conf. Pervasive Comput. Commun.*, 2011, pp. 197–204.
- [34] A. Kosba, A. Saeed, and M. Youssef, "RASID: A robust WLAN device-free passive motion detection system," in *Proc. IEEE Int. Conf. Pervasive Comput. Commun.*, 2012, pp. 180–189.
- [35] A. Saeed, A. E. Kosba, and M. Youssef, "Ichnaea: A low-overhead robust WLAN device-free passive localization system," *IEEE J. Sel. Topics Signal Process.*, vol. 8, no. 1, pp. 5–15, Feb. 2014.
- [36] F. Adib, Z. Kabelac, D. Katabi, and R. C. Miller, "3D tracking via body radio reflections," in *Proc. 11th Conf. Netw. Syst. Des. Implementation*, 2014, pp. 317–329.
- [37] N. Patwari, L. Brewer, Q. Tate, O. Kaltiokallio, and M. Bocca, "Breathfinding: A wireless network that monitors and locates breathing in a home," *IEEE J. Sel. Topics Signal Process.*, vol. 8, no. 1, pp. 30–42, Feb. 2014.
- [38] Y. Wang, J. Liu, Y. Chen, M. Gruteser, J. Yang, and H. Liu, "E-eyes: Device-free location-oriented activity identification using fine-grained WiFi signatures," in *Proc. 20th Annu. Int. Conf. Mobile Comput. Netw.*, 2014, pp. 617–628.
- [39] A. Eleryan, M. Elsabagh, and M. Youssef, "Synthetic generation of radio maps for device-free passive localization," in *Proc. IEEE Global Telecommun. Conf.*, 2011, pp. 1–5.



Chenren Xu received the BE degree in automation from the Shanghai University, in 2008, and the MS degree in applied mathematical statistics, in 2014, and the PhD degree in electrical and computer engineering from the Rutgers University. He is currently an assistant professor in the School of Electronics Engineering and Computer Science and also a member of the Center for Energy-efficient Computing and Applications (CECA), Peking University. His current research interests are in internet-of-things architecture,

mobile cloud computing, and connected health. He was a postdoctoral research fellow in the School of Computer Science, Carnegie Mellon University, from 2014 to 2015.



Bernhard Firner received the master's degree from the Stevens Tech., in 2005, and worked on embedded avionics systems at the ITT Avionics for more than a year before leaving to work toward the PhD degree at the Rutgers University. After receiving the PhD degree, in 2013, he began working with a startup company creating low-power wireless networks for environmental monitoring while also working as an instructor at the Rutgers University. His research investigates the challenges faced by low power wireless networks that must operate for a decade on small coin cell batteries.



Yanyong Zhang is currently a professor in the Electrical and Computer Engineering Department, Rutgers University. She is also a member of the Wireless Information Networks Laboratory (WINLAB). Her current research interests include sensor networks and pervasive computing. Her research is mainly funded by the US National Science Foundation, including the US National Science Foundation (NSF) CAREER award. He is a member of the IEEE.



Richard E. Howard received the BSc degree in physics from Cal Tech (6/70) as well as the PhD degree (1/77) in applied physics from the Stanford University. He is currently the chief technical officer of the Inpoint Systems, Inc., and a research professor at the WINLAB, Rutgers University. Before this, he spent 22 years in the Research Area at Bell Labs, where he worked on a wide range of topics from quantum effects in nanostructures to machine learning, retiring in 2001 as vice president, Wireless Research. His current joint projects with the Rutgers University include developing a new class of wireless nodes for inventory tracking and ubiquitous sensor networks. He is a senior member of the IEEE, and a fellow of both the American Association for the Advancement of Science and the American Physical Society.

▷ **For more information on this or any other computing topic, please visit our Digital Library at www.computer.org/publications/dlib.**